Late-time phase transition and the galactic halo as a Bose liquid. II. The effect of visible matter

S. U. Ji and S. J. Sin
Department of Physics, Hanyang University, Seoul, 133-791, Korea
(Received 28 March 1994)

In a previous work, we investigated the rotation curves of galaxies assuming that the dark matter consists of ultralight bosons appearing in "late-time phase transition" theory. Generalizing this work, we consider the effect of visible matter and classify the types of rotation curves as we vary the fraction of the mass and extension of visible matter. We show that visible matter, in galaxies with flat rotation curves, has a mass fraction 2–10% and it is confined within the distance fraction 10–20%.

PACS number(s): 95.35.+d, 98.62.Gq, 98.80.Cq

I. INTRODUCTION

Recently, motivated by the large scale structure, an ultralight Nambu-Goldstone boson was introduced in dark matter physics under the name of the "late-time cosmological phase transition" [1]. The basic idea of the theory is that if a phase transition happened *after* decoupling, one can avoid the constraint imposed by the isotropy of the microwave background.

Subsequently, one of the authors of this paper [2] tried to apply this idea to the rotation curve of galactic halos. If the phase transition occurred so late, the Universe was already big; therefore the relevant particle must be such that (i) its Compton wavelength provides the scale of interest since there is no other length scale of this kind and (ii) it should be a major component of dark matter [3] to be responsible for the structure formation.

If the dark matter consists of this particle whose mass is, say, $m \sim 10^{-24}$ eV and if the dark matter density in the galaxy is about 10^{-25} g/cm^3, then the interparticle distance is of the order of 10^{-13} cm, while the Compton wavelength is of 10 pc order. Therefore the wave functions of the particles are entirely overlapping and a galactic halo is a giant system of a Bose liquid. In this context, one must consider the dark matter distribution quantum mechanically and this is done in [2].

However, there was a point that had to be clarified further in that work. All the rotation curves obtained there were slightly increasing. While this is consistent with most of the data [4,5], there are a few galaxies whose rotation curves are decreasing. In fact, in [2], the effect of the visible matter was not properly considered. Although most of the mass of a galaxy is attributed to the dark matter, the shape of the rotation curve can depend on the mass profile of the visible matter, especially near the core of a galaxy. In this paper, we consider the effect of the visible matter to the shape of the rotation curve more carefully in the scheme of [2].

We briefly recapitulate the main idea of the paper [2]. The dark matter that consists of an ultralight boson is in a condensation state. Usually bosons condense in the ground state, because in the atomic physics situation matter is always coupled to electromagnetism (cooling) and this efficiently lowers the energy of a system. In our case, however, it was shown [2] that there is no mechanism to reduce the total energy of the system; therefore we look for the nonground state condensation described by a macroscopic wave function that has nodes. We will classify the rotation curves for three thousand different visible matter distributions.

II. QUANTUM FLUID OF DARK MATTER

The system is described by a macroscopic wave function (order parameter) ψ. For simplicity, we consider the spherically symmetric case. We also set the visible matter distribution to be spherically symmetric. This is not realistic, because the visible matter distribution of the disk galaxy is by definition not spherical. However, the purpose of this paper is to show the possibility of the decreasing curves and we believe that, for this purpose, it is enough to consider the spherically symmetric case only. We set the visible matter potential by hand and get the wave function of the total system by numerical work. Also, we neglect interparticle interactions apart from gravity. Since total distribution determines the potential of an individual particle, we expect that the system can be described by a solution of nonlinear rather than linear wave equations.

Newtonian potential V is given by

$$\nabla^2 V = 4\pi G(\rho_{\rm dark} + \rho_{\rm visible})$$

and the Schrödinger equation is

$$i\hbar\partial_t\psi = -\frac{\hbar^2}{2m}\nabla^2\psi + V\psi(r). \tag{1}$$

By identifying $\rho_{\rm dark} = GM_0 m|\psi|^2$ and defining $\rho_{\rm visible} = GM_0 m\rho_v$ we get

$$i\hbar\partial_t\psi = -\frac{\hbar^2}{2m}\nabla^2\psi + GmM_0\int_0^r dr'\frac{1}{r'^2}\int_0^{r'} dr''4\pi r''^2(|\psi|^2 + \rho_v)\psi(r). \tag{2}$$

Here, M_0 is a mass parameter introduced for dimensional reasons. We now set effective density of the visible matters as the Plummer potential for the bulge and exponential decay for the disk. In Eq. (1) it is important to remember that ψ describes the state of the whole system rather than a state of an individual particle. The justification of the nonrelativistic treatment can be found in [2]. The basic idea is $v \sim GmM \sim 10^{-2}$, because in our case $M \sim 10^{12} M_\odot$ and $m \sim 10^{-24}$ eV as we shall see.

In this paper we consider two parameters that determine visible matter distribution. One is the mass ratio of visible matter to dark matter and the other is the distance ratio of the distance in which 90% of visible matter exists to that in which 90% of dark matter exists.

Now we come back to Eq. (1). It is nonlinear, hence we do not have the freedom to normalize the solution. However, as shown in [2] this equation has a scaling symmetry which allows us to resolve the ambiguity due to the choice of M_0. That is, the physical quantity M does not depend on the choice of M_0. We are interested in a stationary solution $\psi(r,t) = e^{-iEt/\hbar}\psi(r)$. We simplify Eq. (1). After scaling by

$$r = r_0\hat{r}\,, \quad \psi = r_0^{-3/2}\hat{\psi};, \quad \rho_v = {r_0}^{-3}\hat{\rho}_v, \quad E = \frac{\hbar^2}{2m}\epsilon\,, \quad r_0 = \frac{\hbar^2}{2GM_0m^2},$$

we can write (1) in terms of the radial wave function $u(\hat{r})$:

$$\ddot{u}(\hat{r}) + \left(\epsilon - \int_0^{\hat{r}} d\hat{r}'\frac{1}{\hat{r}'}\int_0^{\hat{r}'} d\hat{r}''[u^2(\hat{r}'') + \hat{\rho}_v(\hat{r}'')\hat{r}''^2]\right)u(\hat{r}) = 0, \tag{3}$$

where $\hat{\psi}(\hat{r}) = \frac{1}{\sqrt{4\pi}}\frac{u(\hat{r})}{\hat{r}}$. We solve this equation numerically.

III. SCALING ANALYSIS

In Eq. (2) there is a scaling symmetry. That is, Eq. (2) is invariant under the scaling

$$u \to \lambda u, \quad \hat{r} \to \lambda^{-1}\hat{r}, \; \epsilon \to \lambda^2\epsilon, \quad \hat{\rho}_v \to \lambda^4\hat{\rho}_v. \tag{4}$$

Therefore, if $u(\hat{r},\epsilon,\hat{\rho}_v)$ is a solution, so is $\lambda u(\lambda\hat{r},\lambda^2\epsilon,\lambda^4\hat{\rho}_v)$. Let $\hat{M} = \hat{M}_{\rm dark} + \hat{M}_{\rm visible} = \int u^2 d\hat{r} + \int \hat{\rho}\hat{r}^2$. When we scale $\hat{r} \to \lambda^{-1}\hat{r}$, $\hat{M} \to \lambda\hat{M}$. Since $r = r_0\hat{r}$ is a physical quantity, it should be invariant under the scaling. Therefore $r_0 \to \lambda^{-1}r_0$. On the other hand, $r_0 \sim 1/(M_0m^2)$; hence, $M_0m^2 \to \lambda M_0m^2$. The scaling of the normalized velocity $\hat{v}$ can be found as follows. The virial theorem tells us $v^2 = GM/r$, so $v = \sqrt{GM_0/r_0}\sqrt{\hat{M}/\hat{r}} := v_0\cdot\hat{v}$. Therefore under the scaling above, we should get $v_0 \to \lambda^{-1}v_0$ to get the physical velocity $v_0\hat{v}$. On the other hand, $v_0 \sim M_0m$. Hence we get $M_0m \to \lambda^{-1}M_0m$. Summarizing, under the scaling $\hat{r} \to \lambda^{-1}\hat{r}$,

$$M_0m^2 \to \lambda^{-1}M_0m^2,$$
$$M_0m \to \lambda^{-1}M_0m.$$

Therefore m is a scaling invariant while $M_0 \to \lambda^{-1}M_0$. Consequently, $M = M_0\cdot\hat{M}$ is a scaling invariant as it should be.

Why did we do the above analysis? In solving Eq. (2), we must choose the two initial values. One is chosen $\hat{u}(0) = 0$, because $\hat{u}(r)$ is a radial wave function. In the case of a linear Schrödinger equation, there is a freedom of normalization so that one can freely choose the first derivative of u at $r = 0$, or $\psi(0)$. Here, the equation is nonlinear and we do not have the freedom of normalization. We are in trouble unless something happens. It is the scaling symmetry we proved that saved our trouble. In our numerical work, whichever we choose, $\hat{u}_0$ or $\lambda\hat{u}_0$, as the initial value, the physical quantity is not changed. We set $\hat{u}(h) = 0.05 * h$, where h is a small segment of $\hat{r}$.

Now, we set the visible matter distribution as follows:

$$\hat{\rho}_v\hat{r} = \begin{cases} \hat{\rho}_0\cdot\frac{1}{[(\hat{r}/\hat{r}_d)^2+1]^{2.5}} & \text{for the inner bulge,} \\ \hat{\rho}_v(\hat{r}_d)\cdot e^{(\hat{r}_d-\hat{r})} & \text{for the disk.} \end{cases}$$

We study for various values of ρ_0 and $\hat{r}_d$. We classify the rotation curve $[v(r)]$ with the mass and the distance ratio of the visible matter to the dark matter.

IV. COMPARISON WITH OBSERVED DATA

Now we present the main result of this paper. We looked for solutions with five or six nodes. This choice is motivated partly because in this state there is a rotation curve very similar to NGC2998 and NGC801. An additional reason is if we take a node number bigger than 7, the total mass of the halo is larger than $10^{13}M_\odot$. Hence there are some restrictions in our choice. Furthermore, in node numbers 4,3,2,1, the flat region is very narrow, and very hard to classify. So we choose node numbers 5 and 6.

In Fig. 1, we compare NGC2998 and 5.6M–19.7D where 5.6M means the ratio of (visible matter mass) / (total mass) is 5.6% and 19.7D means (90% of visible matter dispersion distance) / (90% of total matter dispersion distance) is 19.7%. There are four ripples in the NGC2998's data. But we suspect that outside the measured region there might still be density peaks and nodes that could lead to further ripples. We can see that the shapes of measured and computed rotation curves are very similar except near the core of the galaxy, where the error of measured data is relatively big. By comparing the maximal velocity and the size of a ripple, we can get v_0 and r_0. By using $m = \hbar/(\sqrt{2}r_0v_0)$ and $M_0 = r_0{v_0}^2/G$, we get $m = 2.90 \times 10^{-24}$ eV and $M_0 = 7.117 \times 10^{11}M_\odot$

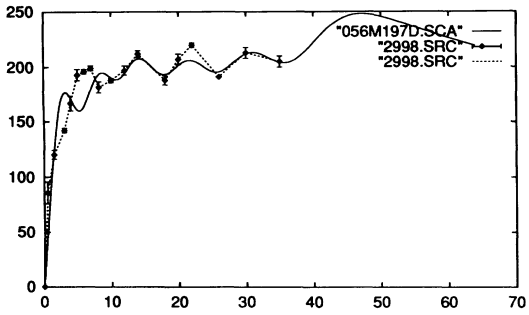

FIG. 1. Comparing the theory and observation for NGC2998 with the data that is 5.6% of the mass fraction and 19.7% of the distance fraction.

in this case.

In Fig. 2, we compare NGC801 and 6.9M–12.7d. In this case $m = 3.14 \times 10^{-24}$ eV and $M_0 = 6.54 \times 10^{11} M_\odot$.

In Figs. 3 and 4, the Y axis is the visible matter's "mass ratio" to total mass, and the X axis is 90% of the visible matter "dispersion distance" to the total distance. Figures 3 and 4 are the classification of the shapes of rotation curves. The slash means that the corresponding rotation curve is increasing; similarly a backslash means decreasing, and a dash means flat. When we measure a rotation curve in a real galaxy, we cannot see the full shape since we can observe only to the extent that a sufficient amount of the hydrogen gas exists. So the up, down, flat (/, \ , —) classifications are not for the full shape, but for the region that corresponds to the first four or five ripples. The figures show that a galaxy with a relatively big visible mass ratio and small extension ratio has decreasing rotation curves, while the one with a small mass ratio and large extension ratio has increasing data. This result is entirely consistent with the observation that compact bright galaxies have decreasing rotation curves and small dwarf galaxies have increasing rotation curves [6].

To give more intuition in reading Figs. 3 and 4, we draw three rotation curves with the same mass ratio and different distance ratios. See Figs. 5–8. We also give rotation curves with the same distance ratio and different mass distance ratios.

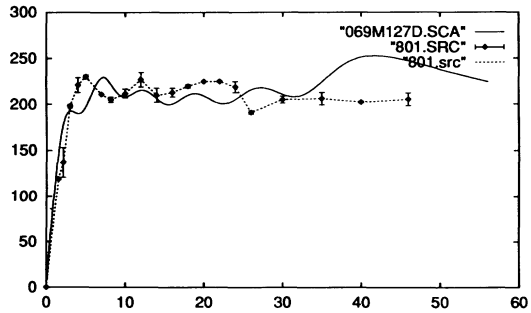

FIG. 2. Comparing the theory and observation for NGC801 with the data that is 6.9% of the mass ratio and 12.7% of the distance ratio.

Notice that we can find some interesting facts on the visible matter distribution from Figs. 3 and 4. Our analysis shows that the flat region is confined in a small window, mass ratio 2–10% and distance ratio 10–20%. On the other hand, the overall flatness is a general phenomenon in the real galaxies. Consequently, in our framework, we can say that most galaxies, which have flat rotation curves, should have the mass and distance ratio in this range.

In Fig. 5, we fix the mass ratio 6.5 ± 0.5 %, and change the rate of dispersion distance. Figure 6 is a node-6 case. As we change the mass fraction of the visible matter, we can find three different types of rotation curves. With the change of the mass fraction, we can obtain various types of rotation curves. If the visible matter distribution is highly confined, the shape of the graph is of a decreasing form. When the visible matter distribution is widely dispersed, the graph is of a slightly increasing form that is very similar to the case of dark matter only. When its distribution is neither very dispersed nor very condensed the graph is almost flat.

In the case shown in Figs. 5 and 6, the mass fraction of visible matter is not as large. So, the shape of the graph is not so different to the case of dark matter only. However, when the mass fraction of visible matter is very large, the situation is quite different. See Figs. 7 and 8.

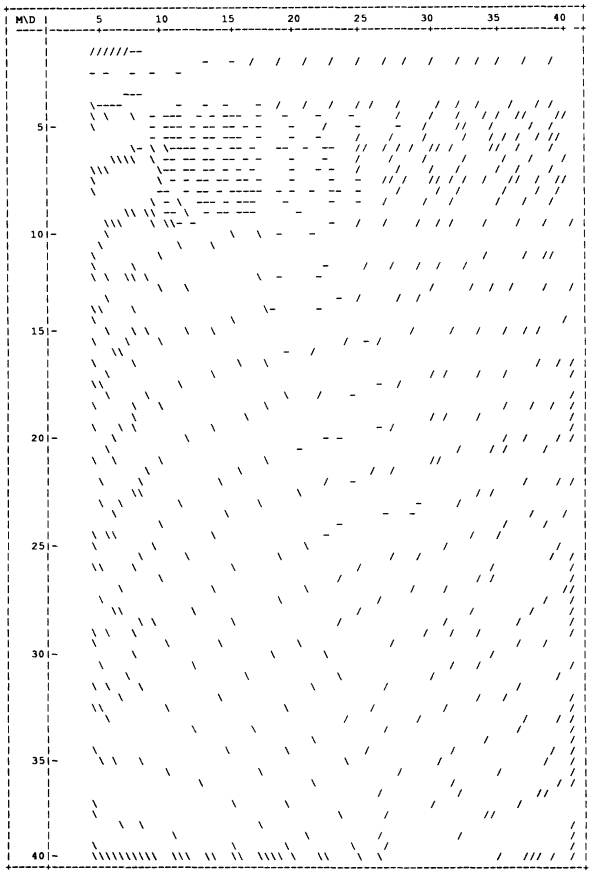

FIG. 3. Classification of node-5 data: / means increasing, — means flat, \ means decreasing rotation curve.

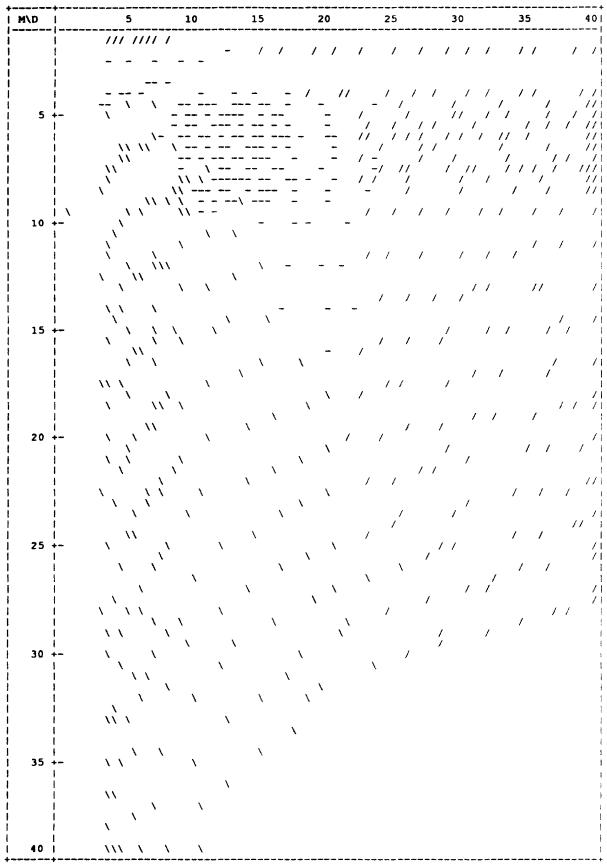

FIG. 4. Classification of node-6 data.

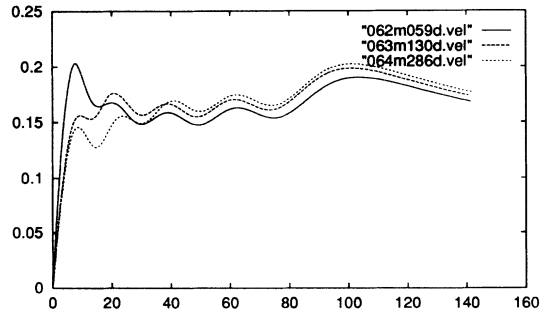

FIG. 5. In Figs. 5–10, (1) means a solid line, (2) means a dashed line, and (3) means a dotted line. (1) Mass ratio = 6.4% and distance ratio = 28.0%; (2) mass ratio = 6.3% and distance ratio = 13.0%; (3) mass ratio = 6.2% and distance ratio = 5.9%, at node 5.

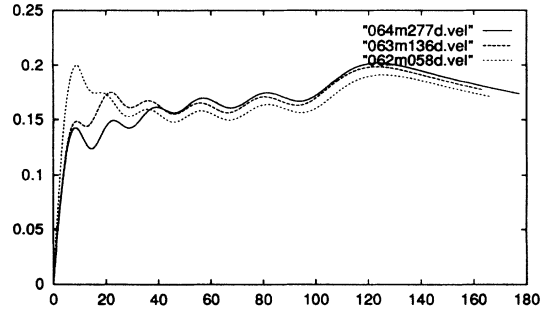

FIG. 6. (1) Mass ratio = 6.4% and distance ratio = 27.7%; (2) mass ratio = 6.3% and distance ratio = 13.6%; (3) mass ratio = 6.2% and distance ratio = 5.8%, at node 6.

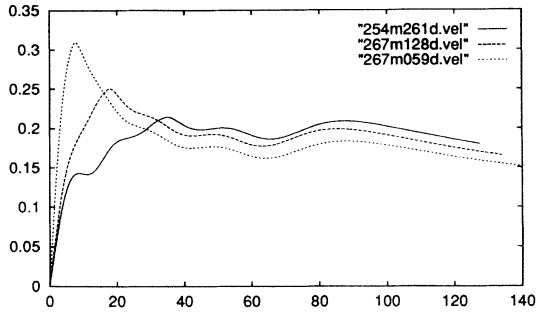

FIG. 7. (1) Mass ratio = 25.4% and distance ratio = 27.4%; (2) mass ratio = 26.8% and distance ratio = 13.8%; (3) mass ratio = 26.8% and distance ratio = 5.9%, at node 5.

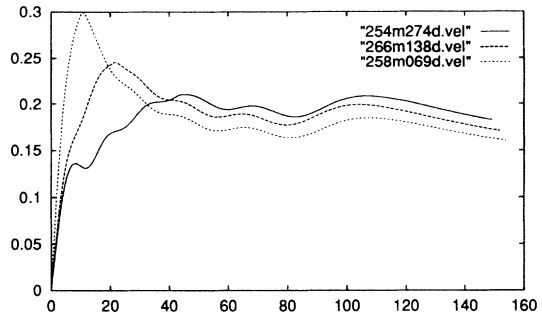

FIG. 8. (1) Mass ratio = 25.4% and distance ratio = 26.1%; (2) mass ratio = 25.8% and distance ratio = 14.3%; (3) mass ratio = 25.8% and distance ratio = 6.9%, at node 6.

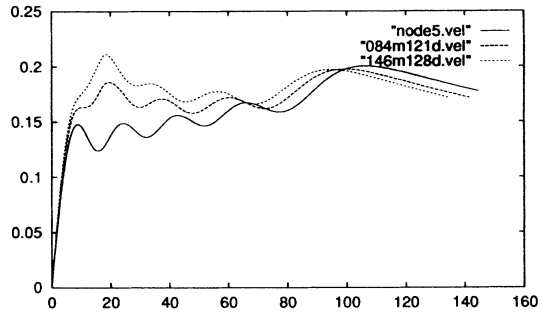

FIG. 9. (1) Mass ratio = 0%; (2) mass ratio = 8.4% and distance ratio = 12.1%; (3) mass ratio = 14.6% and distance ratio = 12.8%, at node 5.

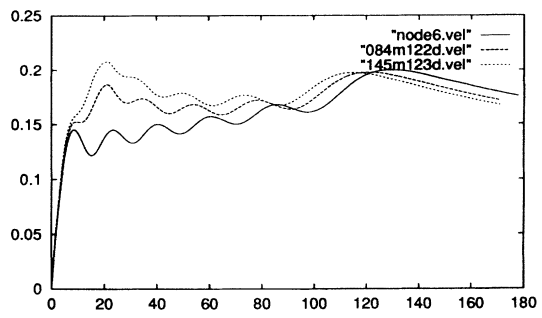

FIG. 10. (1) Mass ratio = 0%; (2) mass ratio = 8.4% and distance ratio = 12.2%; (3) mass ratio = 14.5% and distance ratio = 12.3%, at node 6.

In Fig. 7, we fix the mass ratio $25 \pm 2\,\%$, and change the distance ratio in node 5. The same analysis for node 6 is shown in Fig. 8. Notice that in Figs. 7 and 8 there is no flat curve in any case, and the shapes are quite different to the case of dark matter only.

In Fig. 9, we fix the distance ratio $12 \pm 1\,\%$, and change the mass ratio node-5 case. Figure 10 is for the node-6 case.

V. DISCUSSION AND CONCLUSION

In this paper we investigated the rotation curves of galaxies assuming that the dark matter consists of an ultralight boson appearing in a late-time phase transition. Galactic halos made of this species are a highly correlated Bose liquid. We develop a Landau-Ginzberg-type theory describing the collective behavior of the system.

As the main results, we can obtain decreasing curves as well as flat and slightly increasing curves. In previous work [2] we could see only slightly increasing curves, while observed data show that a few galaxies have decreasing rotation curves. Here we can see the flat curves and the decreasing curves as well by considering the visible matter, in addition to the dark matter. We show that the small amount of dark matter can change the shape of rotation curves near the core significantly.

Our paper has one interesting prediction. The flat case is confined in a rather small window corresponding to the mass ratio $2 \sim 10\,\%$ and in the distance ratio $10 \sim 20\,\%$. On the other hand, one of the observed galaxies has a "flat rotation curve," so we can predict that most of the galaxies have the mass ratio and distance ratio in that region.

So we conclude that the ultralight boson appearing in the late-time phase transition theory has good enough properties to be a dark matter candidate, at least from the rotation curve point of view.

ACKNOWLEDGMENT

This work was supported by the research fund of Hanyang University.

[1] C.T. Hill, D.N. Schramm, and J. Fry, Comments Nucl. Part. Phys. **19**, 25 (1990).
[2] S.J. Sin, preceding paper, Phys. Rev. D **50**, 3650 (1994).
[3] J. Frieman, C. Hill, and R. Watkins, Phys. Rev. D **46**, 1226 (1992).
[4] V. Rubin *et al.*, Appl. J. **289**, 81 (1985); **261**, 439 (1982); **238**, 471 (1980).
[5] V. Rubin, in *Dark Matter in the Universe*, Proceedings of the IAU Symposium, Princeton, New Jersey, 1985, edited by J. Kormendy and G. Knapp, IAU Symposium No. 117 (Reidel, Boston, 1987).
[6] S. Casertano and T.S. van Alberta, in *Baryonic Dark Matter*, edited by D. Lyndell-Bell and Gilmore, NATO ASI Series C, Vol. 306 (Kluwer Academic, Dordrecht, 1990).